



Supplement of

**Performance of the Adriatic Sea and Coast (AdriSC) climate component
– a COAWST V3.3-based one-way coupled atmosphere–ocean
modelling suite: ocean results**

Petra Pranić et al.

Correspondence to: Petra Pranić (pranic@izor.hr)

The copyright of individual parts of the supplement might differ from the article licence.

S1 Introduction

To perform a thorough evaluation of the kilometre-scale Adriatic Sea and Coast (AdriSC) climate ocean model (i.e. ROMS 1-km model), several analyses were carried out but could not all be included in the main text to keep a reasonable article length. The presented supplementary material (Fig. S1 to S9 and text) thus follows the structure and complements the results of the article entitled “Performance of the Adriatic Sea and Coast (AdriSC) climate component – a COAWST V3.3-based one-way coupled atmosphere-ocean modelling suite: ocean results”.

In particular, supplementary results include (a) the spatial analysis depending on 4 depth ranges (i.e. 0-50 m, 50-200 m, 200-500 m and 500-2000 m) of the median absolute deviation (MAD, Fig. S1) associated with the median temperature and salinity biases presented in Figure 2, (b) the monthly and seasonal results (Figs. S2 to S5) for 4 of the 7 subdomains analysed to evaluate the modelled thermohaline properties against the conductivity-temperature-depth (CTD) observations and (c) the monthly and seasonal results (Figs. S6 to S9) for 4 of the 7 acoustic Doppler current profiler (ADCP) and rotor current meter (RCM) datasets used to evaluate the modelled dynamical properties.

S2 Evaluation of the modelled thermohaline properties

The MAD of the temperature and salinity biases depending on the locations of the in situ observations is presented for 4 depth ranges (Fig. S1).

[Figure S1]

In the surface layer (0-50 m), the vertical variability (i.e. the MAD) of temperature biases (Fig. S1.a) is largest in the northern and middle Adriatic, generally ranging from 0.0 – 3.0 °C. In the rest of the Adriatic, the MAD mostly reaches up to 1 °C or slightly above, mainly at some coastal locations. Vertical variability of the salinity biases (Fig. S1.b) is below 0.3 over the entire Adriatic Sea, except in the northern Adriatic and at a few coastal stations. In the upper intermediate layer (50-200 m), the temperature bias MAD is generally below 1 °C, while the salinity bias MAD is mostly under 0.1 in the whole Adriatic. In the lower intermediate (200-500 m) and the deeper (500-2000 m) layers, vertical variability of temperature and salinity biases is very small. MAD of the temperature bias is mostly lower than 0.3 °C, whereas the MAD of the salinity bias is generally close to 0.0.

In this section, the 4 subdomains (i.e. middle Adriatic, Kvarner Bay, Dalmatian Islands and Otranto-Ionian, Fig. 1b) not presented in the main article are analysed in detail.

[Figure S2]

For the middle Adriatic subdomain (Fig. S2), the AdriSC ROMS 1-km demonstrates great capability in reproducing the monthly temperature climatology, except in December when the difference reaches $0.5\pm 0.1^{\circ}\text{C}$ (Fig. S2.a). Salinity is also well captured with slightly lower modelled values up to 0.1 ± 0.0 in January, July and October (Fig. S2.b). Seasonally, negative temperature biases are present near the surface for all seasons except winter when the bias is slightly positive (Fig. S2.d). In summer, temperature biases reach down to -1.0°C near surface but become positive below 20 m. In autumn, temperature is mostly underestimated by the model throughout the water column, while in spring negative biases change the sign under 100 m. Temperature in winter is slightly overestimated at all depths. Concerning the salinity, biases are mostly underestimated at the surface, except in summer at 5 m and below, where there is an overestimation up to almost 0.2 (Fig. S2e). Under 40 m, salinity biases are negative with the largest underestimations in autumn (below -0.1). The analysis of the T-S diagrams shows that the model performs well for all seasons, except in summer when the underestimation of temperature and overestimation of salinity in the surface layer can be clearly seen as the overestimation of PDA (Potential Density Anomaly; hereafter referred as density) below 26 kg m^{-3} (Fig. S2.g, S2.h).

40

[Figure S3]

For the Kvarner Bay subdomain (Fig. S3), concerning the monthly climatology (Fig. S3.a), the AdriSC ROMS 1-km model reproduces temperatures better during winter, spring and autumn (biases around $0.1-0.5\pm 0.0-0.3^{\circ}\text{C}$) than during summer (biases reaching up to $2.0\pm 0.9^{\circ}\text{C}$), similarly to the northern Adriatic subdomain. Salinity is captured relatively well with higher biases (around $0.1-0.5\pm 0.0-0.2$) in March, May, June and December (Fig. S3.b). The seasonal analysis shows small positive temperature biases occurring in winter in the first 25 m of depth, but become quasi null below 25 m (Fig. S3.d). Vertical profiles of temperatures are best reproduced in autumn when the biases are quite small. In spring, temperature is mostly overestimated under 10 m with biases growing with depth and surpassing 0.5°C . In summer, negative temperature biases are found in the surface and large overestimations occur below 20 m of depth reaching around 1.5°C . Salinity is overestimated for all seasons in the whole water column with biases being higher in surface. Unlike for temperature, the best results for salinity are obtained in summer and spring with small biases under 20 m of depth (Fig. S3.e). In autumn and winter at 5 m depth, when the largest number of observations were recorded (Fig.S3.f), the biases reach around 0.3 and 0.4, respectively. Lastly, the seasonal analysis of the T-S diagrams shows that the model performs well independently of the season but with a slightly narrower salinity range, especially for salinity lower than 37.0 (Fig. S3.g, S3.h). The densest waters are well captured, which is important as the Kvarner Bay subdomain is a known dense water formation site (Mihanović et al., 2013; Janeković et al., 2014; Benetazzo et al., 2014, Vilibić et al., 2016; Denamiel et al., 2021).

55

[Figure S4]

For the Dalmatian Islands subdomain (Fig. S4), similarly to the Kvarner Bay subdomain, the AdriSC ROMS 1-km model seems to be capable to reproduce the temperature monthly climatology (Fig. S4.a) for all the months, except from July to

September when modelled values are significantly higher (up to $0.7-2.0\pm 0.4-0.9^{\circ}\text{C}$). Modelled salinities have slightly lower values throughout the year, especially in summer and autumn with biases down to -0.2 ± 0.0 (Fig. S4b). Seasonal analysis of the temperature shows that the largest biases occur in summer, being negative in the first 10 m of depth but positive in the deeper layers, where they reach up to 1.0°C at 30 m of depth (Fig. S4.d). In autumn, the biases are negative in the first 40 m of depth and positive below. Spring and winter both have small biases throughout the water column. Salinity biases are largest in winter and spring in the surface. Below 10 m of depth, the highest underestimations occur in summer and autumn (Fig. S4.e). The analysis of the T-S diagrams shows that the model performs well for all seasons. However, as for the other subdomains, the model overestimates the densities under 25 kg m^{-3} (Figs. S4.g, S4.h).

[Figure S5]

Finally, for the Otranto-Ionian subdomain (Fig. S5), the analysis of the monthly climatology reveals that the temperature and salinity values are well captured by the AdriSC ROMS 1-km model with slightly negative differences during the most of the year for both variables (down to $-0.4\pm 0.3^{\circ}\text{C}$ and -0.1 ± 0.0 , respectively; Figs. S5.a, S5.b). Seasonally, the largest variations of temperature happen in the first 200 m of depth with the highest biases in summer (Fig. S5.d). Below 200 m, the biases are similar for all seasons with values around -0.2°C all the way down to 1000 m of depth. Salinity biases are largest between 100 and 200 m of depth reaching under -0.1 for all seasons except summer (Fig. S5e). Below this depth the biases reduce and approach 0.0 at 600 m of depth, below which they become positive. The analysis of the T-S diagrams shows that the model captures well the seasonal distributions of the water masses. However, for salinities lower than 37.5 and density lower than 25 kg m^{-3} , the modelled values slightly overestimate the observations.

S3 Evaluation of the modelled dynamical properties

In this section, the 4 datasets (i.e. JP1, IOR_Pal_ADCP, NAdEx_ADCP and EACE, Fig. 1c) not presented in the main article are analysed in detail.

80

[Figure S6]

For the JP1 dataset (Fig. S6), AdriSC ROMS 1-km seems to mostly underestimate the observed current speed climatology by $-0.02\pm 0.01\text{ m s}^{-1}$ on average (Fig. S6.a). The current direction differences vary largely from February to July, while from August to January, when the number of observations is significantly larger (Fig. S6.c), the differences are small and reaching up to $17\pm 17^{\circ}$ (Fig. S6.b). Concerning the seasonal variations, the vertical profiles reveal that the model systematically underestimates the observed speed throughout the water column (Fig. S6.d). The smallest biases are present in winter and spring, reaching around 0.01 m s^{-1} and 0.02 m s^{-1} on average, respectively. In summer and autumn, the biases reach around 0.03 m s^{-1} and 0.04 m s^{-1} on average, respectively. The rose plots of the modelled and observed current direction show that the

observed distributions are similarly reproduced by the model for all seasons. In summer and autumn, the southeastward and northwestward current directions are overestimated, while the westward direction is slightly underestimated.

90

[Figure S7]

First, it should be noticed that the IOR_Pal_ADCP dataset (Fig. S7) has a gap in the observations in January and February (Fig. S7.c). For the rest of the year, the AdriSC ROMS 1-km model mostly underestimates the observed current speed by $-0.03 \pm 0.01 \text{ m s}^{-1}$ on average (Fig. S8a). The current direction (Fig. S7.b) is also generally underestimated by $-42 \pm 29^\circ$ to $-8 \pm 22^\circ$. Seasonal vertical profiles of the modelled and observed current speed (Fig. S7.d) show an underestimation of observations for all seasons. Lowest biases are present in winter and summer, reaching 0.03 m s^{-1} and 0.02 m s^{-1} on average, respectively. The highest current speed biases are in spring and autumn, on average around 0.05 m s^{-1} and 0.04 m s^{-1} , respectively. The current direction rose plots (Fig. S7.e) reveal that the model overestimates the occurrences of the main eastward and south-eastward current directions, while other directions are mostly underestimated, independently of the season.

95

[Figure S8]

For the NAdEx_ADCP dataset (Fig. S8), the AdriSC ROMS 1-km model properly reproduces the observed current speed with very small differences throughout the year, except in January and November when they reach up to $0.02 \pm 0.00 \text{ m s}^{-1}$ (Fig. S8.a). Additionally, in this dataset, no observations were recorded in September and October (Fig. S8.c). The current direction monthly climatology (Fig. S8.b) reveals relatively small differences, except in August and December when they reach down to $-62 \pm 17^\circ$. Regarding the seasonal variations, the vertical profiles of the modelled speeds are slightly underestimating the observed speeds by 0.01 m s^{-1} on average, except in autumn when the biases reach around 0.02 m s^{-1} . The rose plots (Fig. S8e) show that the observed current direction distributions are well reproduced by the model with small differences independently of the season.

105

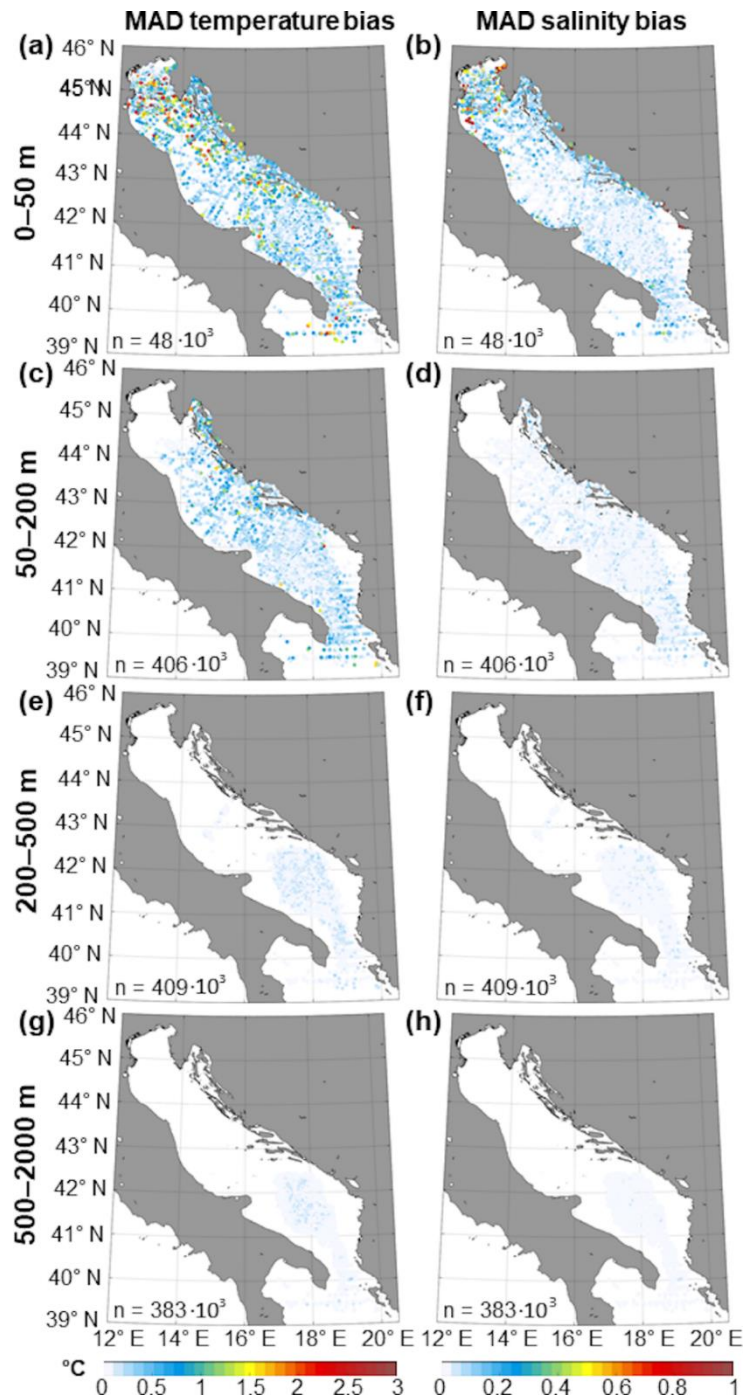
[Figure S9]

Lastly, the EACE dataset (Fig. S9) has a large gap in the observations from July to October (Fig. S9.c). For the rest of the year, the AdriSC ROMS 1-km model overestimates the observed current speed by up to $0.04 \pm 0.02 \text{ m/s}$ in winter, only $0.02 \pm 0.00 \text{ m s}^{-1}$ in December and underestimates down to $-0.01 \pm 0.00 \text{ m s}^{-1}$ in spring (Fig. S8a). The current directions (Fig. S8.b) are largely underestimated in January and February by $-112 \pm 79^\circ$ and $-119 \pm 10^\circ$, respectively. On the other hand, the direction differences are significantly smaller and positive in spring whereas negative in autumn. Seasonal vertical profiles of the modelled and observed current speeds (Fig. S8.d) confirm the overestimation of observations in winter reaching 0.03 m s^{-1} , on average as well as a slight underestimation in spring up to 0.01 m s^{-1} . Finally, the current direction rose plots (Fig. S8e) reveal that the model underestimates in winter and overestimates in spring, the occurrences of the main northwestward current direction.

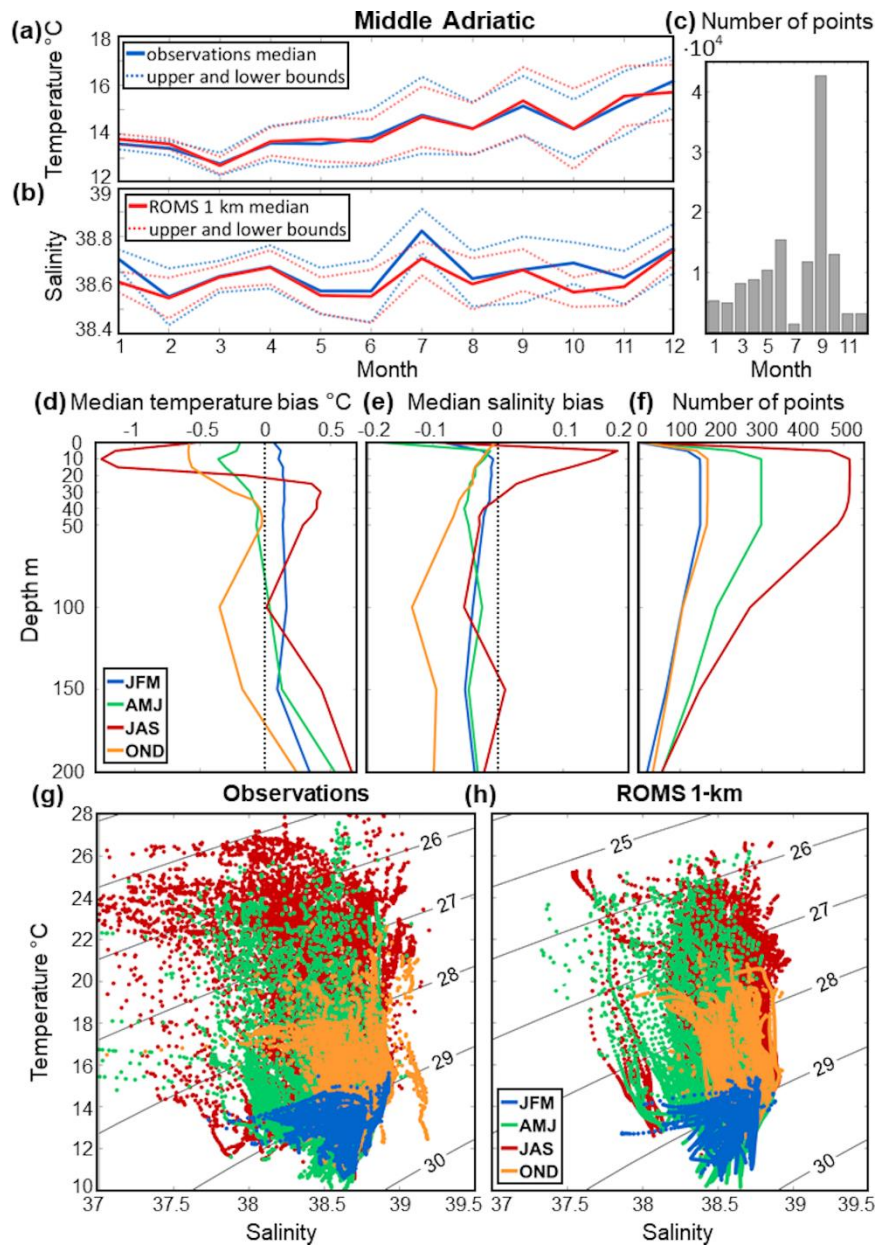
115

References

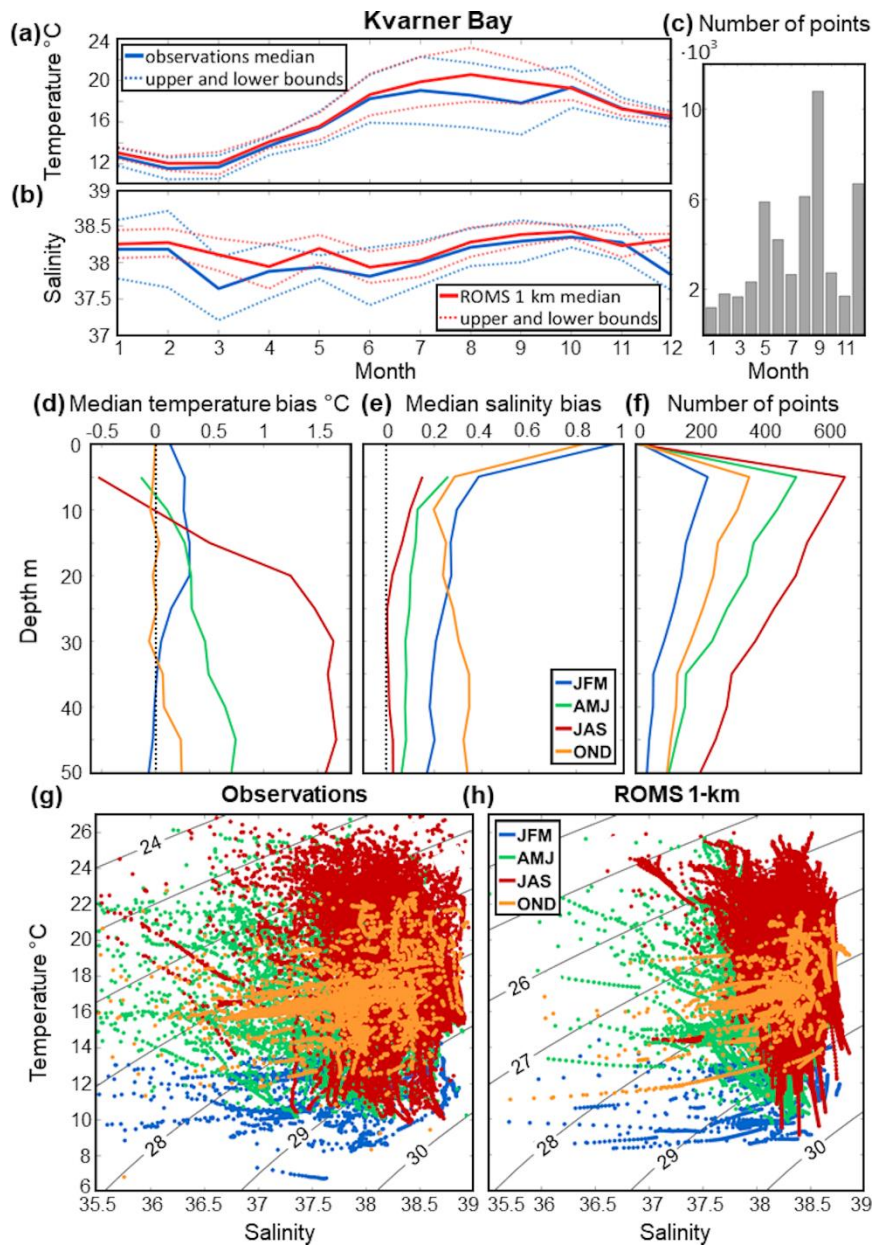
- 120 Benetazzo, A., Bergamasco, A., Bonaldo, D., Falcieri, F.M., Sclavo, M., Langone, L., and Carniel, S.: Response of the Adriatic Sea to an intense cold air out- break: Dense water dynamics and wave-induced transport. *Prog. Oceanogr.* 128, 115–138, doi: 10.1016/j.pocean.2014.08.015, 2014.
- Denamiel, C., Tojčić, I., and Vilibić, I.: Balancing accuracy and efficiency of atmospheric models in the northern Adriatic during severe bora events, *J. Geophys. Res. Atmos.*, 126, e2020JD033516, doi:10.1029/2020JD033516, 2021.
- 125 Janeković, I., Mihanović, H., Vilibić, I., and Tudor, M. : Extreme cooling and dense water formation estimates in open and coastal regions of the Adriatic Sea during the winter of 2012, *J. Geophys. Res. Oceans*, 119, 3200–3218, doi:10.1002/2014JC009865, 2014.
- Mihanović, H., Vilibić, I., Carniel, S., Tudor, M., Russo, A., Bergamasco, A. Bubić, N., Ljubešić, Z., Viličić, D., Boldrin, A., Malačić, V., Celio, M., Comici, C., and Raicich, F. : Exceptional dense water formation on the Adriatic shelf in the winter of 2012, *Ocean Sci.*, 9, 561–572, doi:10.5194/osd-9-3701-2012, 2013.
- 130 Vilibić, I., Mihanović, H., Janeković, I., and Šepić, J.: Modelling the formation of dense water in the northern Adriatic: sensitivity studies, *Ocean Model.*, 101, 17–29, doi:10.1016/j.ocemo.d.2016.03.00, 2016.



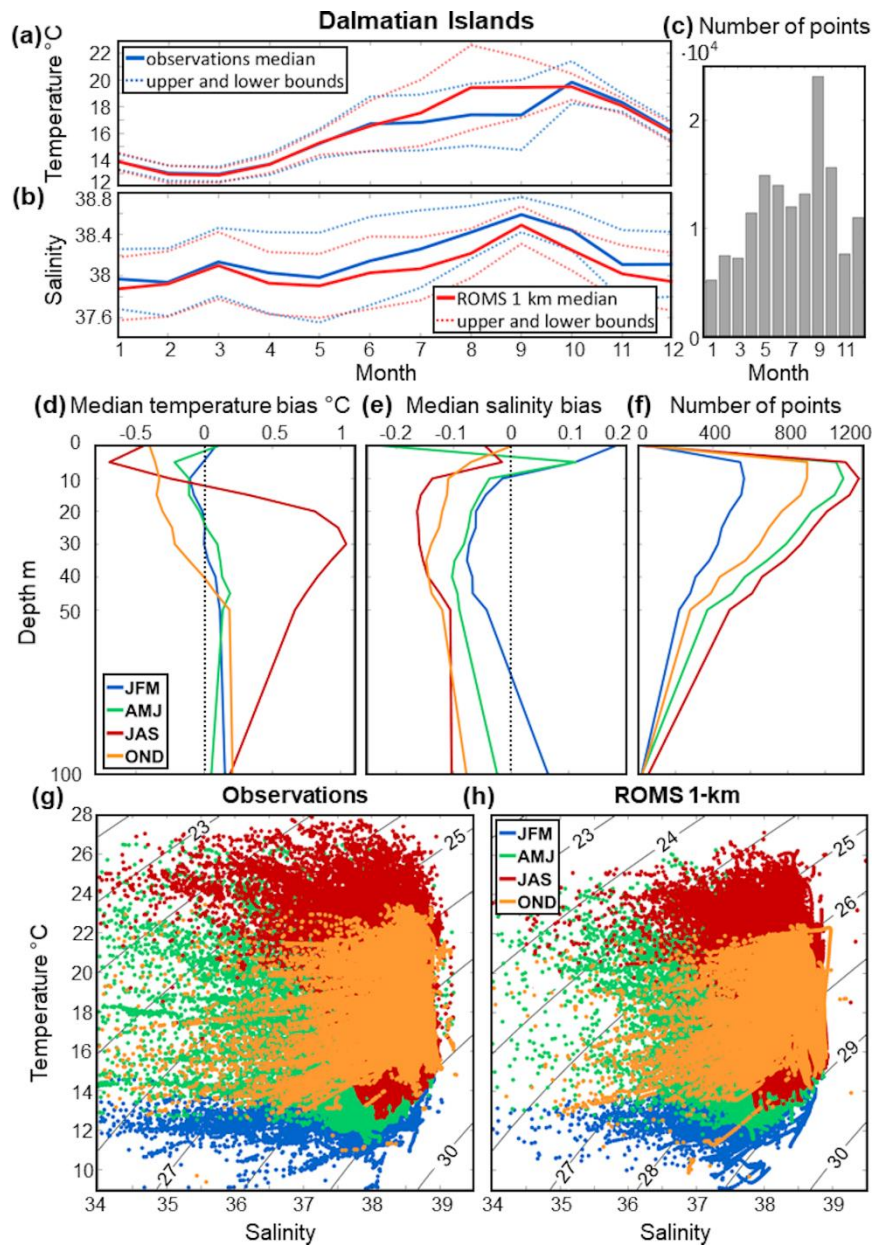
135 **Figure S1. MAD of the temperature (left panels) and salinity (right panels) biases between AdriSC ROMS 1-km model results and CTD observations for depth ranges: (a, b) 0-50 m, (c, d) 50-200 m, (e, f) 200-500 m, (g, h) 500-2000 m, with the total number of points n (bottom left corner).**



140 **Figure S2. Middle Adriatic subdomain. Monthly climatology of AdriSC 1-km and *in situ* (a) median temperature, (b) median salinity and their variabilities (i.e. upper and lower bounds defined as \pm MAD) as well as (c) number of observations per month. Seasonal variations of the (d) temperature and (e) salinity biases between the AdriSC ROMS 1-km model and observations depending on the depth as well as (f) number of observations per depth. Seasonal T-S diagrams for (g) the CTD observations and (h) the AdriSC ROMS 1-km model with Potential Density Anomaly (PDA) isolines.**

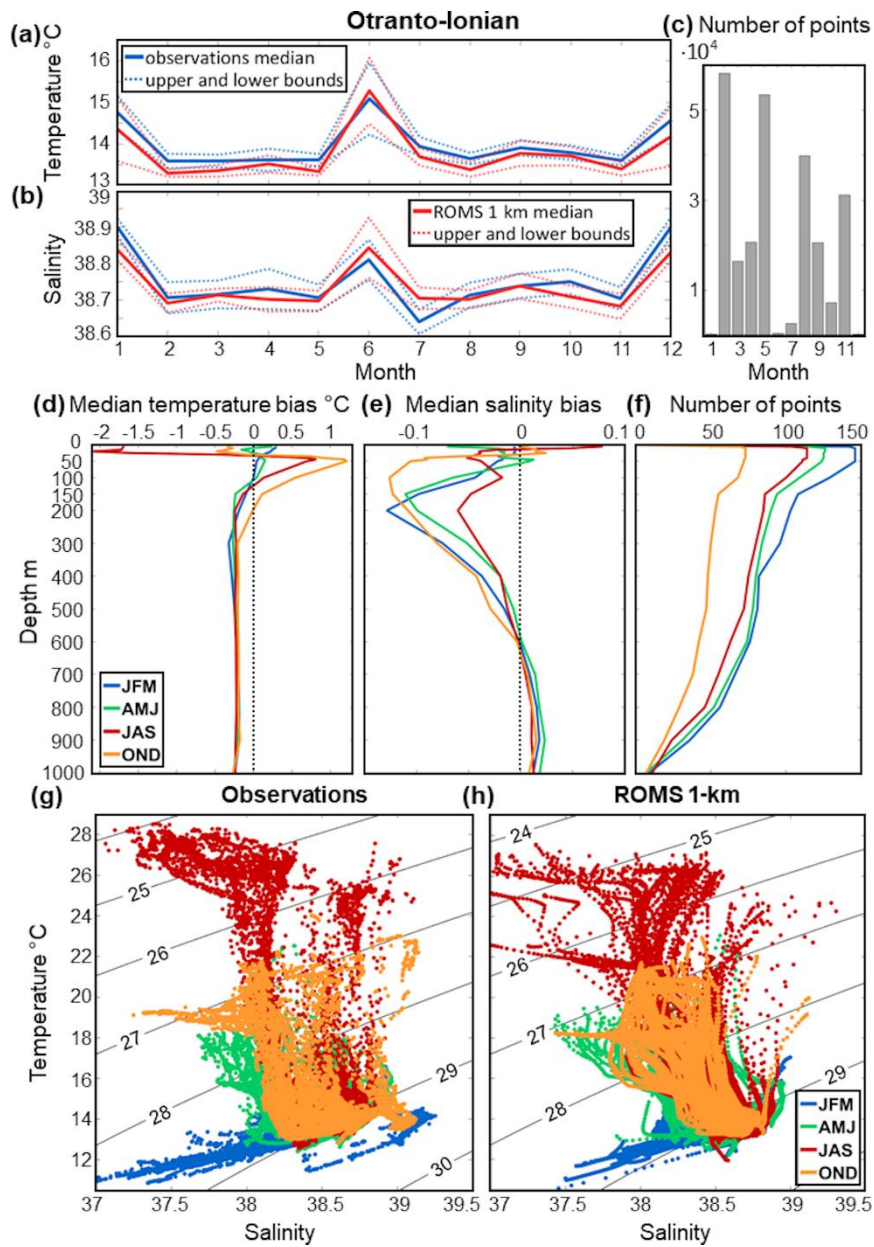


145 **Figure S3. Kvarner Bay subdomain. Monthly climatology of AdriSC 1-km and *in situ* (a) median temperature, (b) median salinity and their variabilities (i.e. upper and lower bounds defined as \pm MAD) as well as (c) number of observations per month. Seasonal variations of the (d) temperature and (e) salinity biases between the AdriSC ROMS 1-km model and observations depending on the depth as well as (f) number of observations per depth. Seasonal T-S diagrams for (g) the CTD observations and (h) the AdriSC ROMS 1-km model with PDA isolines.**



150

Figure S4. Dalmatian Islands subdomain. Monthly climatology of AdriSC 1-km and *in situ* (a) median temperature, (b) median salinity and their variabilities (i.e. upper and lower bounds defined as \pm MAD) as well as (c) number of observations per month. Seasonal variations of the (d) temperature and (e) salinity biases between the AdriSC ROMS 1-km model and observations depending on the depth as well as (f) number of observations per depth. Seasonal T-S diagrams for (g) the CTD observations and (h) the AdriSC ROMS 1-km model with PDA isolines.



155 **Figure S5. Otranto-Ionian subdomain. Monthly climatology of AdriSC 1-km and in situ (a) median temperature, (b) median salinity and their variabilities (i.e. upper and lower bounds defined as \pm MAD) as well as (c) number of observations per month. Seasonal variations of the (d) temperature and (e) salinity biases between the AdriSC ROMS 1-km model and observations depending on the depth as well as (f) number of observations per depth. Seasonal T-S diagrams for (g) the CTD observations and (h) the AdriSC ROMS 1-km model with PDA isolines.**

160

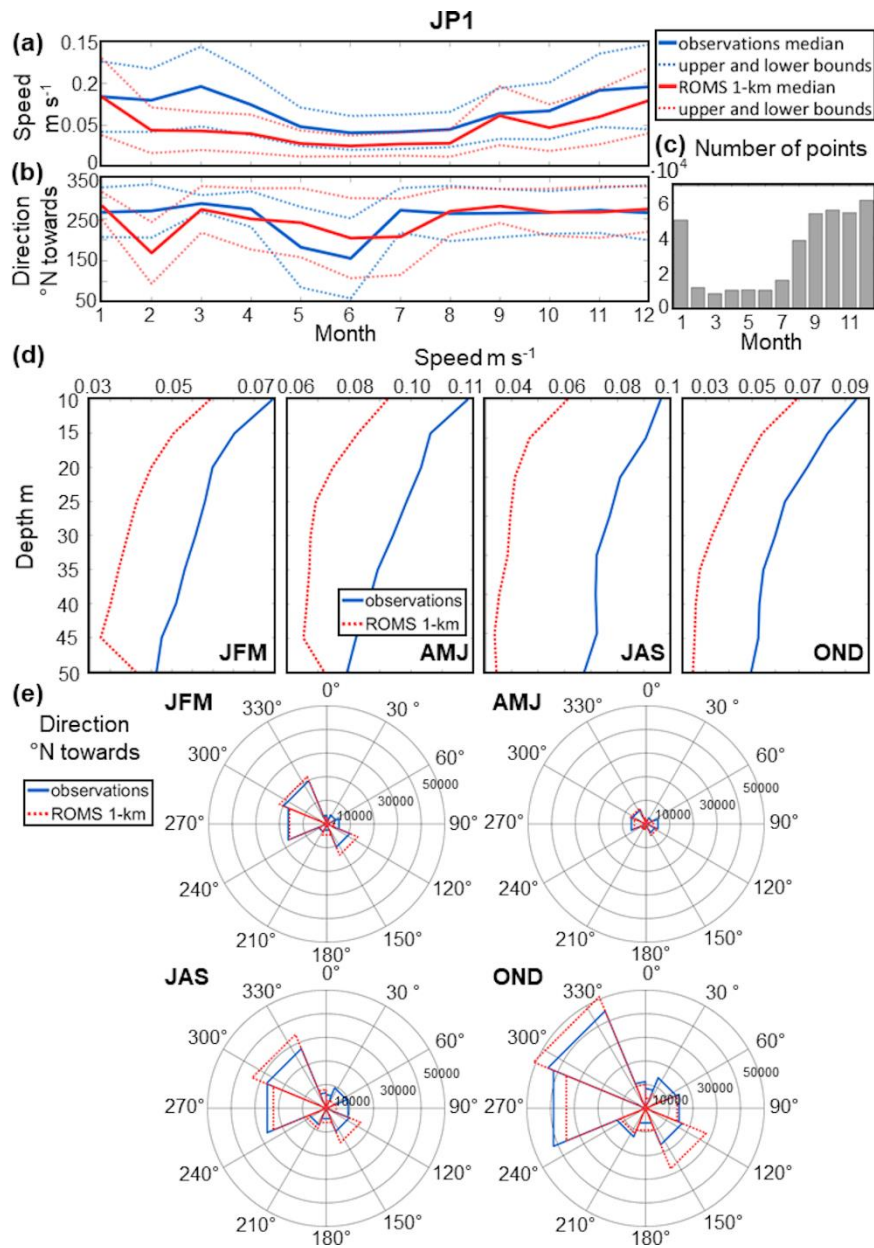


Figure S6. JP1 dataset. Monthly climatology of AdriSC 1-km and *in situ* (a) median speed, (b) median direction and their variabilities (i.e. upper and lower bounds defined as $\pm\text{MAD}$) as well as (c) number of observations per month. Seasonal variations of the (d) speed of AdriSC ROMS 1-km model and observations depending on the depth. Seasonal rose plots of the (e) direction for ADCP observations and the AdriSC ROMS 1-km model.

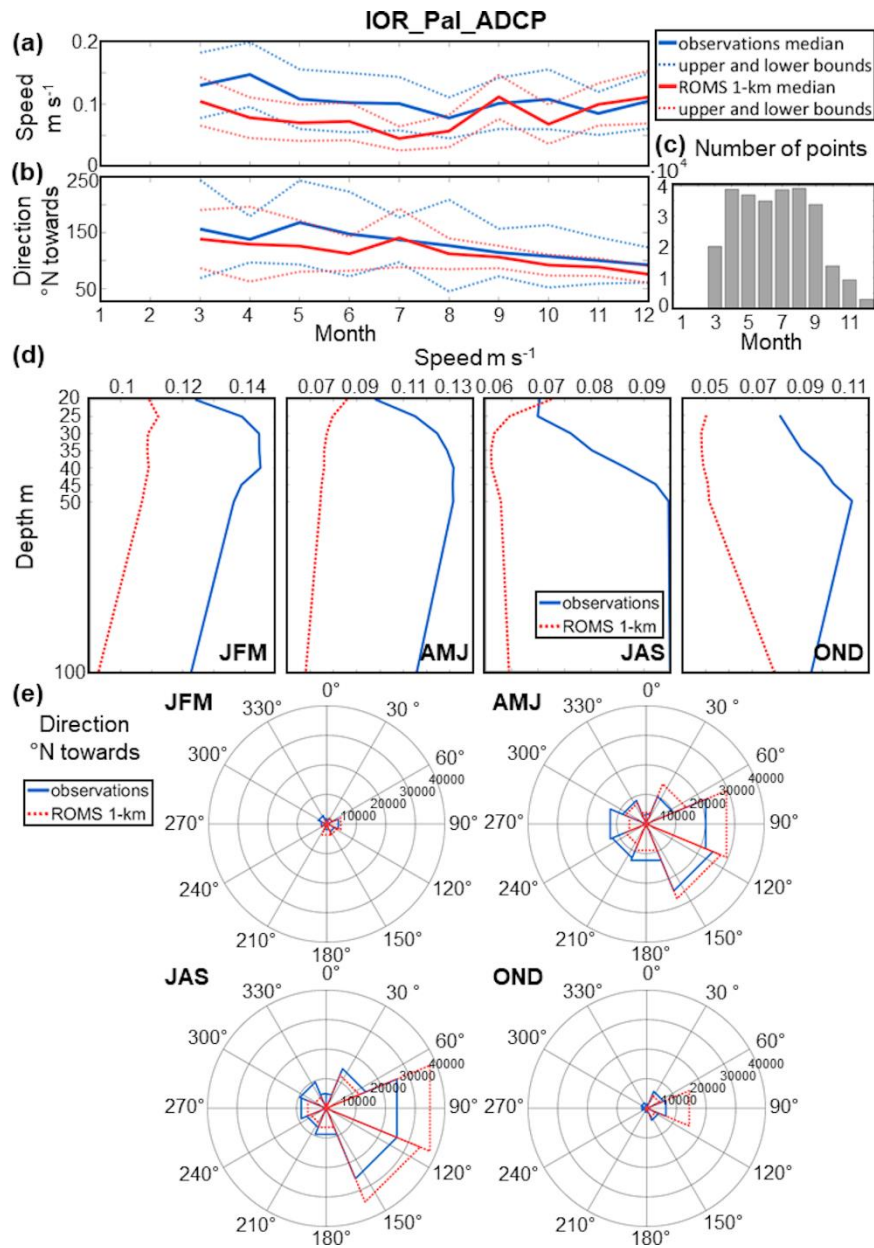


Figure S7. IOR_Pal_ADCP dataset. Monthly climatology of AdriSC 1-km and *in situ* (a) median speed, (b) median direction and their variabilities (i.e. upper and lower bounds defined as $\pm\text{MAD}$) as well as (c) number of observations per month. Seasonal variations of the (d) speed of AdriSC ROMS 1-km model and observations depending on the depth. Seasonal rose plots of the (e) direction for ADCP observations and the AdriSC ROMS 1-km model.

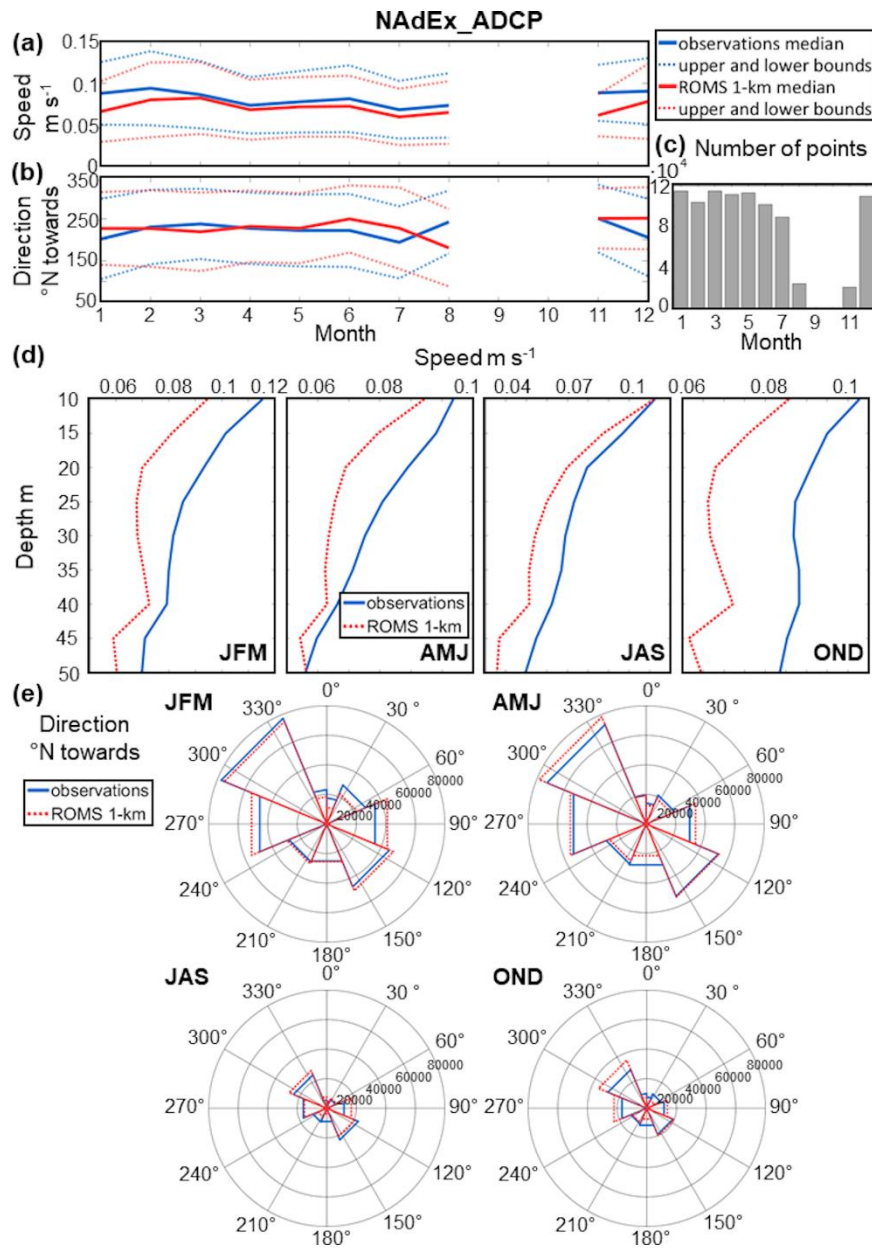


Figure S8. NAdEx_ADCP dataset. Monthly climatology of AdriSC 1-km and *in situ* (a) median speed, (b) median direction and their variabilities (i.e. upper and lower bounds defined as $\pm\text{MAD}$) as well as (c) number of observations per month. Seasonal variations of the (d) speed of AdriSC ROMS 1-km model and observations depending on the depth. Seasonal rose plots of the (e) direction for ADCP observations and the AdriSC ROMS 1-km model.

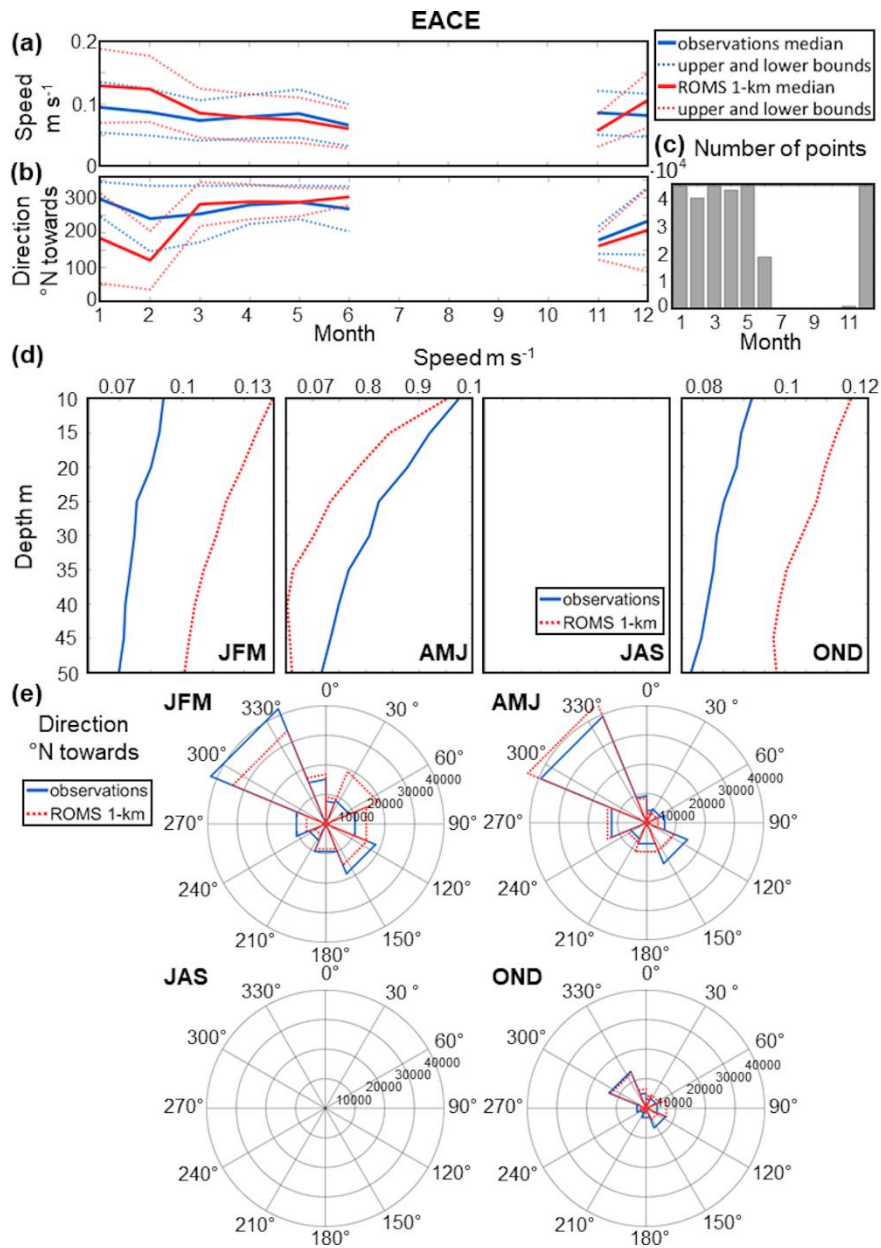


Figure S9. EACE dataset. Monthly climatology of AdriSC 1-km and *in situ* (a) median speed, (b) median direction and their variabilities (i.e. upper and lower bounds defined as $\pm\text{MAD}$) as well as (c) number of observations per month. Seasonal variations of the (d) speed of AdriSC ROMS 1-km model and observations depending on the depth. Seasonal rose plots of the (e) direction for ADCP observations and the AdriSC ROMS 1-km model.

180